


## Agricultural development has not necessarily caused forest cover decline in semi-arid northern China over the past 12,000 years

Qian Hao<sup>1</sup>, Yue Han<sup>2</sup>, Hongyan Liu<sup>2</sup>   & Ying Cheng<sup>3</sup>

Forest cover significantly affects the global carbon cycle, biodiversity, and human welfare, but is seriously threatened by human activities. Here we found that anthropogenic forces did not necessarily lead to forest cover decline in the marginal agricultural region of northern China based on a quantitative reconstruction of 12,000-years forest cover changes using modern analog technique and random forest. The forest cover was strongly affected by human activities in the core agricultural region, as indicated by the high independent effects of archeological sites (38.3%) and burning area (42.3%). In contrast, climate impacted the forest cover in the marginal agricultural region, where the annual precipitation and summer mean temperature contributed 52.4% and 27.4%, respectively. Agricultural development in the marginal agricultural region likely occurred in the river valley or sunny slopes, not overlapping with zonal forests growing on shady slopes. This study implies much less afforestation potential than previously expected in the marginal agricultural region.

<sup>1</sup>Institute of Surface-Earth System Science, School of Earth System Science, Tianjin University, Tianjin, China. <sup>2</sup>College of Urban and Environmental Sciences, and PKU-Saihanba Station, Peking University, Beijing, China. <sup>3</sup>School of Geography and Tourism, Shaanxi Normal University, Xi'an, China. email: [lhy@urban.pku.edu.cn](mailto:lhy@urban.pku.edu.cn)

Forest cover changes directly affect the global carbon budget, biodiversity, hydrological properties, and ecosystem functions<sup>1–6</sup>. Increasing the forest cover is regarded as a mechanism for carbon sequestration and mitigating climate change<sup>7,8</sup>. Global afforestation has promoted forest cover<sup>9,10</sup>, and semiarid regions such as the marginal agricultural region in northern China have been recommended for potentially massive afforestation projects<sup>11,12</sup>. In addition, increasing afforestation efforts in this region could provide important ecological services, such as controlling desertification and soil erosion. Although some countries and regions have put efforts to increase forest cover<sup>13–16</sup>, forest cover has declined globally<sup>17</sup>. Deforestation and forest degradation pose challenges to human health and economic development<sup>18,19</sup>.

Drivers of forest cover decline vary regionally and change over time<sup>20–22</sup>, but human activities are consistently key drivers<sup>23</sup>. Increased agricultural conversion and plantation development have played an important role in natural forest cover decline, especially in developing countries during recent years<sup>24–26</sup>. Fires caused by climate or human activities may contribute to approximately 59% of forest cover losses in boreal forests<sup>27</sup>. On the other hand, in ecologically vulnerable areas such as vegetation ecotones, forests often show a high sensitivity to climate change<sup>28,29</sup>. The relative impacts of human activities and climate change on forest cover changes remain controversial. To solve this debate, long-term reconstructions (centennial and millennial-scale) of forest cover dynamics are essential to clarify the main drivers<sup>30–32</sup>.

Agricultural development in northern China has a history of more than ten thousand years<sup>33–36</sup>. Two agricultural civilizations, the Yellow River Civilization and the West Liao River Civilization, dominated human activities in northern China. The agricultural civilizations started to develop or bloom approximately 8000 cal yr BP in both civilizations<sup>37</sup>, while the development of pastoralism remarkably influenced the human societies in the West Liao River region during the late-Holocene with the climate cooling (Supplementary Table 1)<sup>38–41</sup>. Forced by climate change, there was a process of advance and retreat between agricultural and pastoral civilizations in northern China<sup>38,39,42</sup>. Previous studies have found that agricultural development, such as burning

activities, has affected the forest cover of northern China since 8000 cal yr BP<sup>43</sup>. In contrast, climate change, such as the weakening and strengthening of the Asian summer monsoon, has also played a key role in forest cover changes<sup>44–47</sup>. However, a quantitative estimation of the impacts of climate change and human activities on the evolution of forest cover, which is critical to afforestation policies in this region, is still lacking.

In this study, we explored the forest cover evolution since the Holocene and discussed the driving factors in northern China. The pollen-forest cover relationship was constructed by correlating the pollen percentages of surface soil and modern forest cover data, and then the absolute 12,000-years forest cover was reconstructed with the pollen spectra of sedimentary profiles by using the modern analog technique and the random forest (RF)<sup>48–50</sup>. The 30 sediment profiles were divided into two groups based on the current vegetation distribution. The 15 sediment profiles on the northwestern part belonged to the marginal agricultural region with the minimum precipitation of about 100 mm currently, while those ( $n = 15$ ) on the southeastern part dominated with farmland belonged to the core agricultural region with the maximum precipitation of more than 500 mm currently (Fig. 1). Finally, we summarized the spatiotemporal patterns and quantified the driving factors of 12,000-years forest cover changes in northern China by comparing climatic and human activity parameters. This study found that the human activities affected forest cover during the mid-Holocene in northern China, but this influence was limited to the core agricultural region. Climate determined the evolution of forest cover in the marginal agricultural region because forests preferred to grow at high altitudes on shady slopes, which did not overlap with farming depending on river valleys and sunny slopes; thus, the development of agricultural civilization in this region does not necessarily require the sacrifice of forests.

## Results

**Spatiotemporal changes of forest cover.** In terms of evolution, the average forest cover of northern China gradually increased in the early Holocene (Fig. 2a). It peaked in the mid-Holocene (the

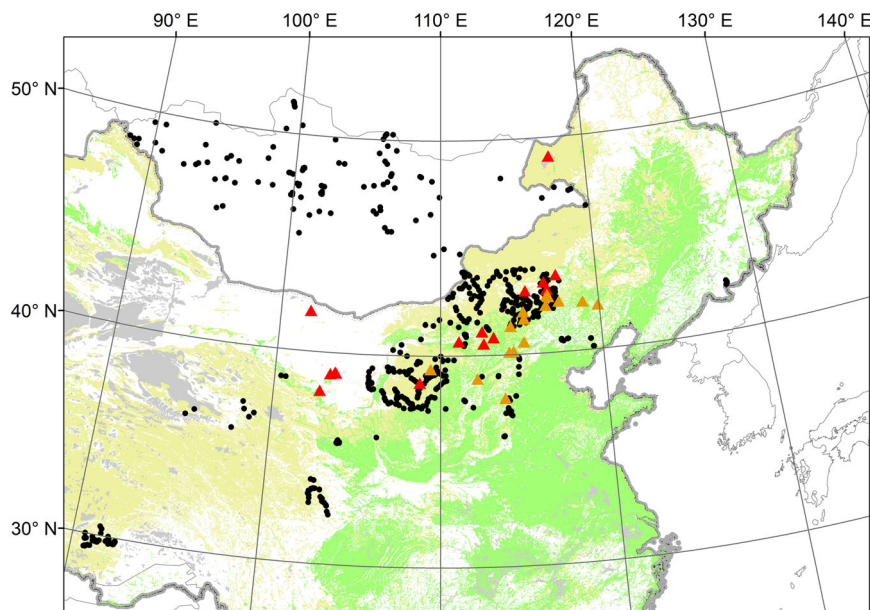


**Fig. 1 Sedimentary profiles in northern China, surface soil pollen sites and the distribution of modern farmland and grassland.** The red triangles indicate sedimentary profiles belonging to the marginal agricultural region, and the orange ones belong to core agricultural region. The black dots indicate the surface soil pollen sites ( $n = 769$ ). Green area indicates farmland, while yellow area indicates grassland.

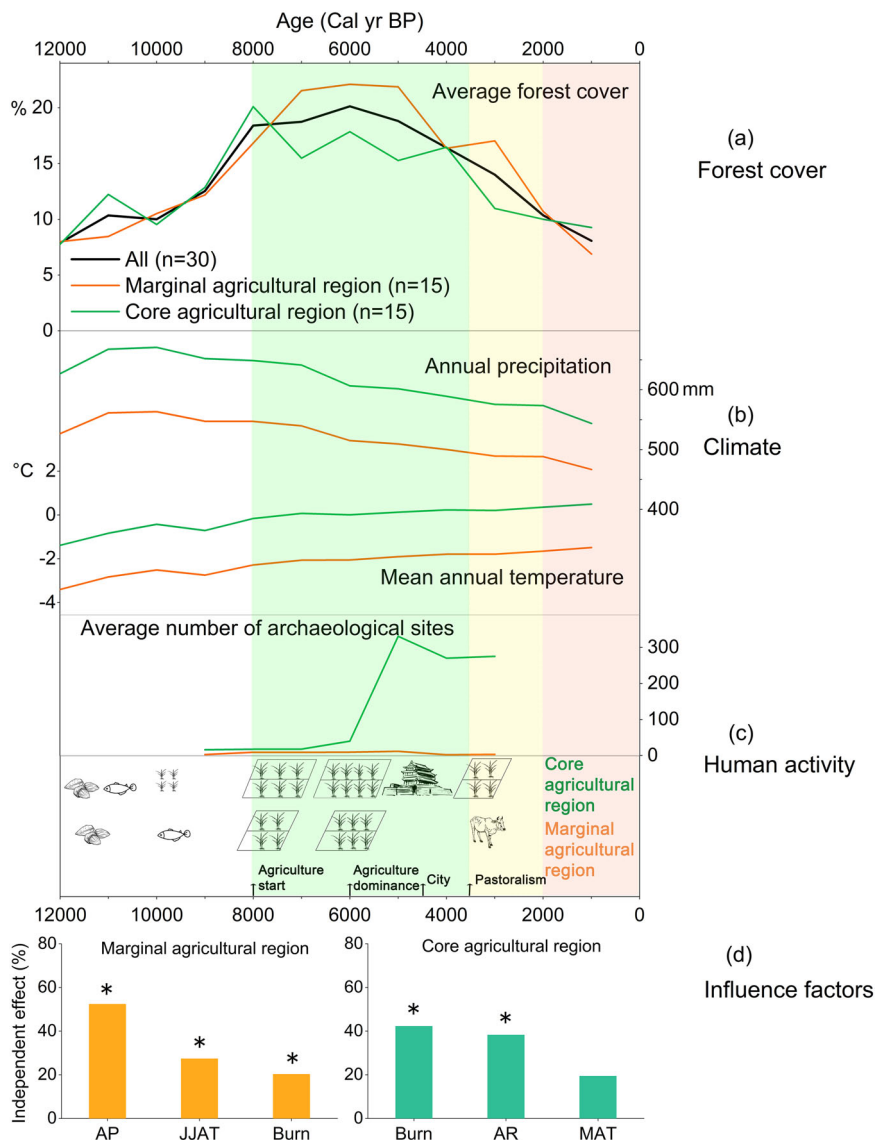


**Fig. 2 Changes in forest cover, climate and human activities in the marginal agricultural region and core agricultural region in northern China since the Holocene.** Changes in forest cover **a**, climate **b** and human activities **c** in the marginal agricultural region and core agricultural region in northern China since the Holocene. The independent effects of the influencing factors on forest cover in these two subregions are shown below **d**. JJAT (the mean temperature of June, July, and August) indicates the mean monthly summer temperature, while AP indicates the annual precipitation; both are selected as the indexes of climate. AR and Burn indicate the number of archeological sites and burning areas in the basin of the sedimentary profile, respectively. “\*” indicates significance at the level of 0.05.

regional average was approximately 20%) and gradually decreased to approximately 10% in the late Holocene (Figs. 2a and 3). Based on the forest cover changes and human activities, four stages were identified (Fig. 2a, c): From 12,000 to 8000 cal yr BP, the average forest cover increased significantly; from 8000 to 3500 cal yr BP, the forest cover in the marginal agricultural region first increased and then decreased but remained high for the entire period, while that in the core agricultural region decreased gradually; after approximately 3500 cal yr BP, both subregions showed descending trends, while the decreasing rate was relatively large in the marginal agricultural region from 2000 cal yr BP to present (Fig. 2a).

In terms of internal spatial differences, although the forest cover of the two subregions generally exhibited the same trend over time, the forest cover of the core agricultural region was higher than that of the marginal agricultural region during 12,000–8000 cal yr BP and lower than that of the marginal agricultural region during 8000–2000 cal yr BP, although the

significance level was higher than 0.05 (Fig. 2a). The average forest cover in core agricultural region exceeded that in the marginal agricultural region again around 2000 cal yr BP (Figs. 2a and 3).

**Determinants of forest cover evolution.** As shown in Figs. 2 and 3, the annual precipitation (AP) and mean annual temperature (MAT) were both relatively high in the core agricultural region (Fig. 2b). The number of archeological sites in northern China gradually increased after 9000 cal yr BP, peaked from 5000 to 4000 cal yr BP and slightly decreased thereafter. The number of archeological sites in the core agricultural region was higher than that in the marginal agricultural region during the whole period, indicating that the intensity of human activities in the core agricultural region was higher (Figs. 2c and 3).

To further quantify the impacts of climate and human activities on forest cover in the marginal agricultural region and core

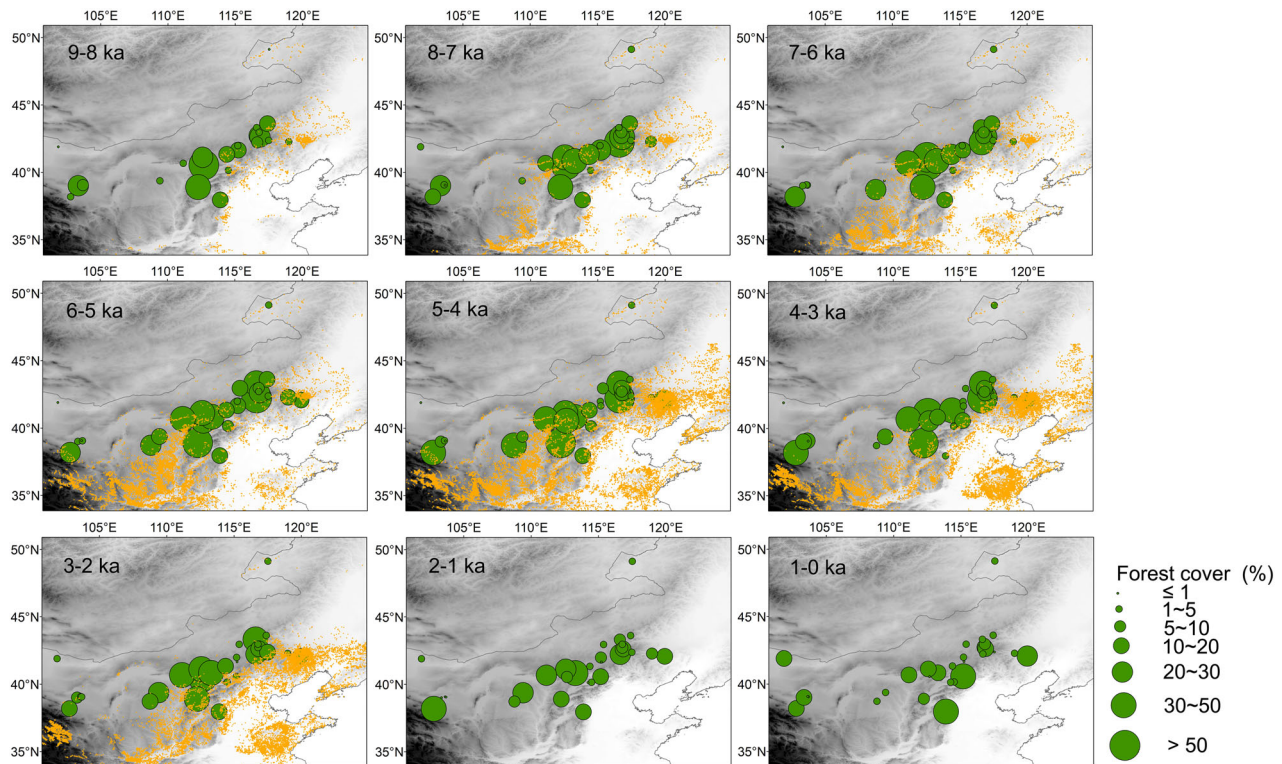


**Fig. 3** Forest cover and the changes of archeological sites in northern China from 9000 to 0 cal ka BP. “ka” represents millennium. The size of the green circles indicates forest cover values. The yellow dots indicate the archeological sites<sup>53</sup>, representing the spatio-temporal patterns of human disturbance.

agricultural region from 8000–2000 cal yr BP, which was the period with both agricultural and pastoral civilizations (Fig. 2c). As mentioned above, the MAT, mean monthly summer temperature (the mean temperature of June, July and August: JJAT) and the AP were selected as indicators of climate factors. The number of archeological sites (AR) in the sediment profiles of the basin were selected as indicators of the intensity of human activities, while the fire intensification (Fire) and the burning area (Burn) could be parameters of both climate and human activities. Based on the variables selected by the Akaike information corrected criterion (AICc), an optimal generalized linear model was established as follows:

Marginal agricultural region:  $\ln(\text{forest cover}) = 0.003560\text{AP} + 0.1676\text{JJAT} - 373.4\text{Burn} - 1.684$ ,  $R^2 = 55.20\%$

Core agricultural region:  $\ln(\text{forest cover}) = -0.003645\text{AR} - 1029\text{Burn} - 0.4605\text{MAT} + 3.824$ ,  $R^2 = 19.50\%$

Based on the hierarchical partitioning analysis with the above selected parameters, the AP was the dominant factor affecting forest cover, and the independent effect was 52.4% in the marginal agricultural region. The JJAT and the burning area also had a significant impact, reaching 27.4% and 20.3%, respectively (Fig. 2d). In the core agricultural region, the burning area and the number of archeological sites were the dominant factors affecting forest cover (42.3 and 38.3%, respectively), but the effect of the MAT was not significant (Fig. 2d).

## Discussion

Our results show that the forest cover was high during the 8000–4000 cal yr BP (Fig. 2a), and the dynamics were indeed affected by human activities, as indicated by the high independent effects of AR and Burn (Fig. 2d) in the core agricultural region, especially during the period of agricultural civilization. In contrast, climate change, but not human activities, impacted the forest cover changes in the marginal agricultural region (Fig. 2d).

The different climate and civilization development stages determine the forest cover spatiotemporal pattern (Fig. 4). From 12,000–8000 cal yr BP, an agricultural civilization did not emerge in the marginal agricultural region or bloom in the core agricultural region, and the human activities indicated by archeological sites were not intense<sup>51,52</sup>. The forest cover was mainly affected by climate for both the two subregions (Fig. 4). After 8000 cal yr BP, slash-and-burn was the main production mode of primitive agriculture<sup>53,54</sup>, and the core agricultural region was more susceptible to this impact than the marginal agricultural region (Fig. 4), resulting in a decline in forest cover, although the wetter climate during this period promoted a high forest cover, ultimately causing the forest cover in the core agricultural region to be lower than that in the marginal agricultural region. During the next stage, the marginal agricultural region was mainly affected by pastoralism because climate drying led to agricultural recession (Supplementary Table 1)<sup>41,55</sup>, which had a relatively weak impact on forest cover (Fig. 4). In contrast, the core agricultural region was still mainly affected by agriculture; thus, the forest cover in the core agricultural region was lower than that in the marginal agricultural region (Fig. 4). Until 2000 cal yr BP, the forest cover in the core agricultural region with a relatively warmer and wetter climate was higher than that in the marginal agricultural region (Fig. 4). The parameters collected in this study, such as archeological data, were not enough to quantify the main driver to the forest cover evolution for both subregions. However, both human population and human activities (i.e., agriculture, pastoralism) rose up dramatically after 2000 cal yr BP, no matter in the marginal agricultural region or the core agricultural region<sup>56,57</sup>; thus, we deduced that the human activities played an important role on forest evolution. Besides, wars in the history of Chinese dynasties could destroy the natural forest greatly since soldiers need wood to make weapons and build camps, especially in recent centuries. The soldiers also burnt the natural grasses to

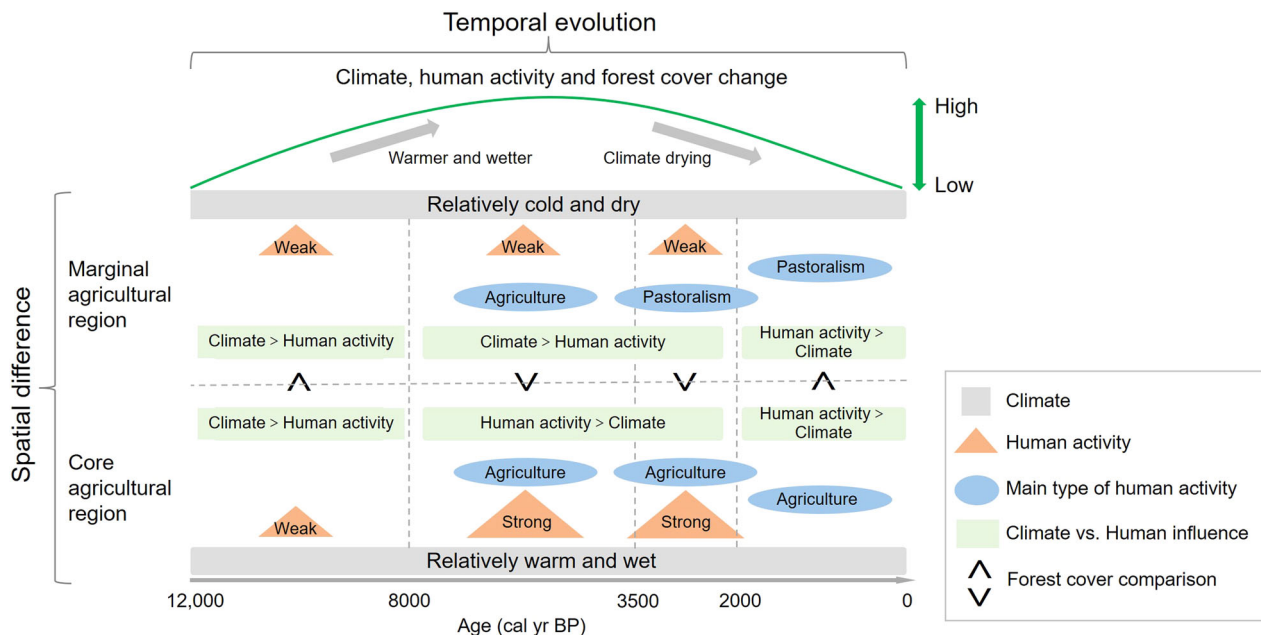


**Fig. 4 Model of the temporal and spatial evolution of 12,000-years forest cover in the study area.** The climate change, intensity of human activity, and main type of human activity are all shown. The comparisons of forest cover and the main influencing factors between the two subregions are illustrated by “>” or “<”.

defend enemy attack<sup>58</sup>. In general, human activities, probably exceeding climate, profoundly affect forest dynamics.

Throughout history, agriculture has often developed at the expense of forests in China<sup>54,59</sup>, especially since the Neolithic period, when farming replaced foraging, which is consistent with the highly negative independent effect of AR on forest cover in our study in the core agricultural region (Fig. 2d). Other human activities, such as fire making<sup>60</sup>, also led to a decline in forest cover<sup>61</sup>. In this study, we also found there was a negative correlation between burning areas and forest cover (Fig. 2d). In other regions, such as Europe, human activities have shown a significant effect on forest cover<sup>62–64</sup>. Early farming economies spread into southeastern Europe approximately 8500 years ago<sup>65</sup>, and temperate forests have declined progressively since approximately 6000 cal yr BP due to the clearing of forests for agriculture in Europe<sup>66</sup>. In summary, as forest cover has evolved in the core agricultural region, the impact of human activities has been greater than that of climate since approximately 8000 cal yr BP (Fig. 4).

However, the climate is the main factor for the evolution of forest cover in the Holocene in the marginal agricultural region no matter in the period dominated by agriculture or pastoralism (Figs. 4 and 5), as indicated by the large independent effects of AP and JJAT (Fig. 2d). During the period dominated by agriculture, agricultural development did not threaten the forest cover on shady slopes at high altitudes during the mid-Holocene (Fig. 5). Flat sunny southern slopes and relatively low altitudes, such as river valleys (Fig. 5)<sup>67–69</sup>, are preferred for farming, and these areas always have better soil conditions. In contrast, forests in the marginal agricultural region are critically dependent on soil humidity; thus, high altitude shady slopes are always characterized by forests (Fig. 5), because the insolation intensities of northern and southern slopes vary greatly, which results in strong differences in the temperature and available moisture<sup>70–72</sup>. Even so, farmers may still disturb the growth of forests by logging or harvesting for timber products, but this effect was limited to local scale rather than large scale clearance of forest. In addition, agricultural and pastoral civilizations successively occurred in northern China during the Holocene<sup>39,42</sup>; overall, the marginal

agricultural region was mainly affected by pastoralism civilization after 3500 cal yr BP<sup>38</sup>. Nomads lived near water and grass, and the pastoral mode of production have had less impact on forest cover in the marginal agricultural region<sup>39,43</sup>, which is different from the core agricultural region. Therefore, climate change surpassed human activities in driving forest cover evolution in the marginal agricultural region of northern China.

Our results suggest that the marginal agricultural region is mainly influenced by climate; thus, future forest management practices should consider climate warming and drying, which could threaten forest growth and lead to forest die-off<sup>73–75</sup>. This fact may also explain why afforestation efforts have not led to a significant increase in forest cover in the marginal agricultural region since the last century<sup>76</sup>. The war around the mid-20th century is indeed another reason for the forest cover decrease in China. Therefore, we decline the widespread afforestation in semiarid areas in China, as recommended to restore the lost forest cover by human activities. However, it is possible to establish drought-tolerant shrubs on a suitable scale according to the appropriate policy “planting shrubs where suitable for shrubs”.

Afforestation is also carried out in the semiarid lands in other regions or counties<sup>77</sup>, which improves soil fertility and carbon storage. However, other studies showed negative effect on local ecosystem health, because the deep-rooted tree species could lead to a significant reduction of groundwater recharge<sup>78</sup>. Therefore, long-term studies (e.g., thousands of years) could provide more information about the forest evolution and scientific references about where and how to conduct afforestation.

### Conclusions

In conclusion, forest cover increased during the early Holocene to the mid-Holocene in northern China and decreased after the mid-Holocene both in the marginal agricultural region and core agricultural region. Human activities showed an enhanced influence on forest cover from 8000 to 2000 cal yr BP, with strong agricultural activities in northern China, but this influence was limited to the core agricultural region. Climate but not human activity determined the evolution of forest cover in the marginal agricultural region because forests prefer to grow at high altitudes

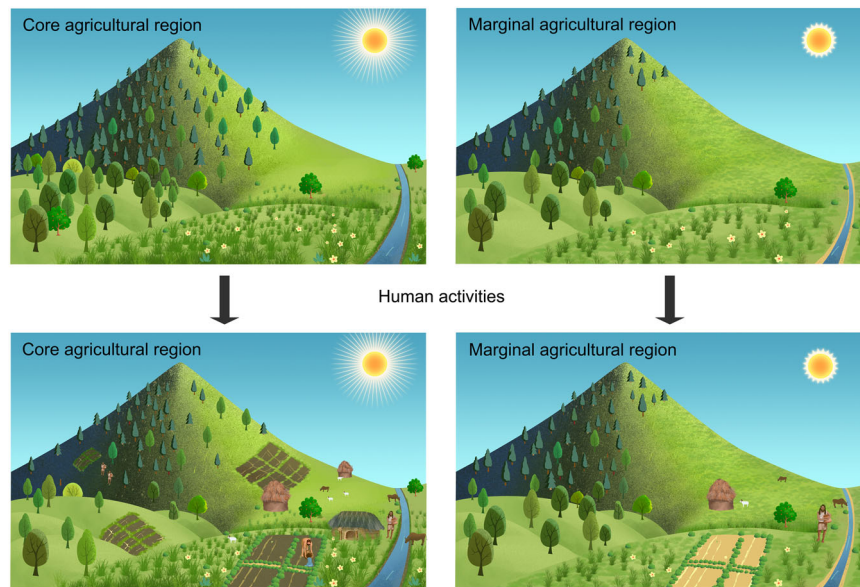


**Fig. 5 Conceptual model of vegetation changes with the development of agricultural civilization.** Climate-determined forest distribution can be extended to different topographies in the core agricultural region, but limited to shady slopes and high altitudes in the marginal agricultural region<sup>100</sup>. For the core agricultural region, humans occupy both the sunny and shady slopes for agriculture. However, agriculture is concentrated in the flat terrain, the sunny south slopes, and the relatively low altitudes due to the better light and soil conditions and the relatively small human populations in the marginal agricultural region, which has less influence on forest cover.

on shady slopes, while farming depends on river valleys and sunny slopes. The development of agricultural civilization in this region does not necessarily require the sacrifice of forests, and the afforestation potential is limited because of future climate drying in the marginal agricultural region.

## Methods

**Study area.** The study area is mainly located in the plateau area of East Asia (37°46′–53°08′N and 87°40′–122°15′E) (Fig. 1). The mean annual precipitation (MAP) in the region ranges from 100 to 600 mm, and the MAT range is relatively large. Winter is cold and long and accompanied by strong winds. Summer is characterized by high temperatures and concentrated periods of precipitation. The northern part of the Mongolian Plateau is mainly affected by the water vapor of the Arctic Ocean, while the eastern part is mainly affected by the water vapor of the Pacific Ocean. With the gradual weakening of the intensity of monsoons from the southeast to the northwest, the MAT and MAP decrease from the southeast to the northwest.

According to the current distributions of pastureland and farmland, the study region was divided into two subregions: marginal agricultural region and core agricultural region. Though the vegetation distribution changes with time, the southeastern part (i.e., core agricultural region) of our study area is dominated by farmland, while the northwestern part (i.e., marginal agricultural region) is characterized by a mixture of pasture and farmland or dominated by pasture. The West Liao River Civilization mainly originated from the marginal agricultural region (Supplementary Table 1)<sup>43</sup>, where is also very sensitive to climate changes<sup>79–81</sup>. As an ecologically fragile area, also serving as an important ecological barrier, this ecotone in northern China, dominated by the semiarid climate, has become a key area for afforestation, sand stabilization and soil retention<sup>82</sup>. The main vegetation is steppe currently (Fig. 1). In contrast, the main vegetation in the core agricultural region, dominated by the semi-humid climate, is temperate forest and farmland. As the origin of the Yellow River Civilization, the production modes of the core agricultural region were dominated by agriculture since approximately 7000 cal yr BP (Supplementary Table 1). This was different from that in the marginal agricultural region, which has undergone agriculture-pastoralism advance and retreat along with climate drying and livestock introduction (Supplementary Table 1)<sup>43</sup>. Therefore, comparisons between these two subregions could help to understand forest cover responses to climate change and human activities.

**Data sources.** The 769 sites of pollen percentages in the surface soil were based on experimental data accumulated by our research group and published data (Supplementary Table 2; Fig. 1). Though many surface soil sites (black dots) are outside China, the vegetation type there is similar with that in the marginal agricultural region of northern China. Besides, modeling process using the modern vegetation and surface soil sites need a large number of sites to get high accuracy; thus, this study retained these sites.

Most of the previous long-term vegetation studies in this region were conducted at least 10 years ago (Supplementary Table 3), and the resolutions of pollen records based on sedimentary profiles were not high enough. To obtain relatively abundant records, a total of 30 pollen spectra with pollen percentage or concentration data of sedimentary profiles were collected and retained (Supplementary Table 3). Generally, the mean sampling resolution was <700 years, the entire record spanned a minimum of 6000 years and the chronology was based on a minimum of two radiocarbon dates. Based on these published pollen data, 55 major terrestrial pollen families or genera were digitized using GetDataW\_2.26 software.

The vegetation cover data used in this study were MOD44B Version 6 Vegetation Continuous Field (VCF) data (<https://doi.org/10.5067/MODIS/MOD44B.006>), which include three vegetation cover components (i.e., tree cover, non-tree cover, and non-vegetated cover (bare)) with a spatial resolution of 250 m. The 2000–2016 yearly data were downloaded, and then 17-year averages were calculated. In ArcGIS software, a circular buffer zone was generated around each sample point in the modern pollen database, and the radius of the buffer zone of the topsoil sample points was set to 5 km<sup>32</sup>. Then, the average tree cover in the buffer zone of each sample point was calculated as the forest cover corresponding to each modern pollen sample point.

Climate index data since the Holocene, such as the monthly average temperature and monthly precipitation data in TraCE-21 ka (from 20,000 cal yr BP to 1989 CE), were used. The spatial resolution is 3.75°, and the temporal resolution is up to one year (<http://www.cgd.ucar.edu/ccr/TraCE/>)<sup>83,84</sup>. The modern climate data were based on the integrated WorldClim data, including the MAT and AP data from 1970 to 2000, with a spatial resolution of 1 km.

To explore the historical influence of human activities in northern China, fire intensification (Fire; infrared radiation intensity emitted by burning per unit area, watt/m<sup>2</sup>) and burning area (Burn; proportion of burning area, %) data in TraCE-21ka were used as indicators of fires during the Holocene to partly indicate the intensity of historical human activities. Because fire could be caused by both climate and human activities as suggested by the previous studies<sup>85,86</sup>, we also collected the archeological data to indicate the intensity of human activities in the basin. The archeological data from the early Neolithic Age to the early Iron Age (c. 8000–500 BC)<sup>53</sup> were plotted in ArcGIS, and the number of archeological sites (AR) within a radius of 50 km from each sediment profile was used in the following calculation.

**Data analysis.** In previous studies, a variety of methods have been proposed and continuously improved to establish the quantitative relationship between pollen and vegetation<sup>87–89</sup>, including the modern analog technique and machine learning method. The regional-scale research has been carried out using the above-mentioned methods to quantitatively reconstruct past vegetation cover and land-use changes<sup>62,64,90–94</sup>, but there is a lack of systematic research on absolute vegetation cover in East Asia<sup>32,54</sup>.

The modern analog technique uses the analogy of modern and past pollen assemblages to quantitatively simulate ancient vegetation and is a common method

used to reconstruct climate changes using pollen data<sup>50</sup>. Among the machine learning algorithms, Sobol and Finkelstein<sup>95</sup> suggested that the random forest (RF) classifier scores highest on all of the metrics used for model evaluations. The RF model is a new machine learning technology<sup>49,96</sup> because it can quickly process multi-variable and nonlinear relationships and handle small samples well, which is increasingly used in ecological research<sup>49,97,98</sup>. It was used to reconstruct vegetation dynamics in the Tibetan Plateau since the Last Glacial Maximum and also proved to have high accuracy<sup>99</sup>. In this study, the modern analog technique and RF were selected to model the forest cover.

The modern analog technique method requires the establishment of a relatively large modern pollen database, and  $k$  samples closest to the pollen assemblage in the profile were searched among the modern pollen samples. The squared chord length of these  $k$  samples was used as the weight to calculate the weighted average of the forest cover corresponding to the  $k$  samples as the forest cover of the sediment profile in a certain period.  $k$  was the value when the root mean square error (RMSE) was the smallest among the 1000 iterations. Additionally, bootstrap sampling was used for verification, and the  $R^2$  values were obtained. This method was implemented in R using the “analog” package.

The two packages in the open-source software R (V 3.3.2; R Development Core Team 2016), Package of “Random Forest” and “Random Forest SRC”, were used in the RF model. The input independent variable was the modern pollen concentration or percentage, and the dependent variables were forest cover and grass cover; using these variables, the corresponding models were established. The out-of-bag (OOB) data (approximately one-third of the samples) were used as test data and were not included in the models, and the error of the model results was then calculated (i.e., the OOB error). This test method can replace cross-validation or unbiased estimation to calculate the error<sup>49</sup>. When modeling, the parameter for random numbers was changed, and 1000 calculation iterations were performed to generate 1000 optimal RF models to make the results more random and objective. Then, pollen concentration or percentage data from the sediment profiles were input, and each model was used to reconstruct past forest and grass cover changes. The results of the 1000 models were averaged to obtain the absolute forest and grass cover changes and the uncertainties.

The forest and grass cover change trends reconstructed by the two methods were relatively consistent based on the results (Supplementary Figs. S1–S3). Because of the relatively large span of longitude and different local site conditions (e.g., altitude, terrain), the forest cover dynamics were different among these sites, even in the same subregion, but the variation characteristics of the whole region can be outlined by data synthesis. A comparison of the results of the two methods showed that for the reconstructed forest and grass cover changes, the  $R^2$  value of the modern analog technique method was higher (Supplementary Table 4); thus, the presented results are mainly based on the modern analog technique.

In this study, MAT (annual mean temperature), JJAT (mean monthly summer temperature, i.e., the mean temperature of June, July, and August), and AP (annual precipitation) were selected as indicators of climate factors. The AR (the number of archeological sites) was selected as indicators of the intensity of human activities. Fire (fire intensification) and Burn (burning area) calculated above in the sediment profiles of the basin could be parameters of both climate and human activities. Based on the results of the Kolmogorov–Smirnov test, the forest cover of the marginal agricultural region ( $P = 0.0299$ ) and core agricultural region ( $P = 0.1088$ ) followed a log-normal distribution. Therefore, the logarithm of the forest cover ( $\ln(\text{forest cover})$ ) was used as the dependent variable, and the six aforementioned indicators were used as independent variables. The combination of the dependent and independent variables for each millennium of each profile represented a sample. The sample sizes of the marginal agricultural region and core agricultural region were 87 and 75, respectively. The Akaike information corrected criterion (AICc) was used to screen the independent variables. Based on the selected variables, the optimal generalized linear models (GLM) for the two subregions were established.

To determine the relative contribution of each independent variable to forest cover changes, the variances of the two models were calculated separately. This method can express the independent contribution of each variable, effectively solving the problem of multicollinearity. These were implemented in R using the “MuMin” and “hier.part” packages.

## Data availability

The raw data of 769 sites of surface soil pollen percentages and 30 pollen spectra of sedimentary profiles are available in the Dryad Digital Repository under the link <https://doi.org/10.6084/m9.figshare.22632679>. The current vegetation cover is MOD44B Version 6 Vegetation Continuous Field (VCF) data (<https://doi.org/10.5067/MODIS/MOD44B.006>). Climate index data, fire intensification (Fire; infrared radiation intensity emitted by burning per unit area,  $\text{watt/m}^2$ ), and burning area (Burn; proportion of burning area, %) data since the Holocene are available in TraCE-21ka (from 20,000 cal yr BP to 1989 CE; <http://www.cgd.ucar.edu/ccr/TraCE/>). The archeological data from the early Neolithic Age to the early Iron Age (c. 8000–500 BC) is referred to Hosner et al. (2016). Other data information can be found in the Supporting Information. Hosner, D., Wagner, M., Tarasov, P. E., Chen, X., & Leipe, C. Spatiotemporal distribution patterns of archeological sites in China during the Neolithic and Bronze Age: An overview. *Holocene* 26, 1576–1593 (2016).

Received: 25 August 2022; Accepted: 21 April 2023;

Published online: 06 May 2023

## References

1. Rotenberg, E. & Yakir, D. Contribution of semi-arid forests to the climate system. *Climate* 327, 451–454 (2010).
2. Baccini, A. et al. Estimated carbon dioxide emissions from tropical deforestation improved by carbon-density maps. *Nat. Clim. Change* 2, 182–185 (2012).
3. Harris, N. L. et al. Baseline map of carbon emissions from deforestation in tropical regions. *Science* 336, 1573–1576 (2012).
4. Alkama, R. & Cescatti, A. Biophysical climate impacts of recent changes in global forest cover. *Science* 351, 600–604 (2016).
5. Chazdon, R. L. et al. Carbon sequestration potential of second-growth forest regeneration in the Latin American tropics. *Sci. Adv.* 2, e1501639–e1501639 (2016).
6. Watson, J. E. M. et al. The exceptional value of intact forest ecosystems. *Nat. Ecol. Evol.* 2, 599–610 (2018).
7. Tong, X. W. et al. Forest management in southern China generates short term extensive carbon sequestration. *Nat. Commun.* 11, 129 (2020).
8. Xu, Y., Zhang, T. Y. & Shao, C. L. Afforestation increases ecosystem productivity and carbon storage in China during the 2000s. *Agr. Forest Meteorol.* 296, 108227 (2021).
9. Potapov, P. et al. Eastern Europe’s forest cover dynamics from 1985 to 2012 quantified from the full landsat archive. *Remote Sens. Environ.* 159, 28–43 (2015).
10. Guo, J., Gong, P., Dronova, I. & Zhu, Z. L. Forest cover change in China from 2000 to 2016. *Int. J. Remote Sens.* 43, 593–606 (2022).
11. Cernansky, R. How to rebuild a forest. *Nature* 560, 542–544 (2018).
12. Liu, H. et al. Nature-based framework for sustainable afforestation in global drylands under changing climate. *Global Change Biol.* 28, 2202–2220 (2022).
13. Piao, S. L. et al. Detection and attribution of vegetation greening trend in China over the last 30 years. *Global Change Biol.* 21, 1601–1609 (2015).
14. Roopsind, A., Sohngen, B. & Brandt, J. Evidence that a national REDD plus program reduces tree cover loss and carbon emissions in a high forest cover, low deforestation country. *P. Natl. Acad. Sci. USA* 116, 24492–24499 (2019).
15. Heilmayr, R., Echeverria, C. & Lambin, E. F. Impacts of Chilean forest subsidies on forest cover, carbon and biodiversity. *Nat. Sustain.* 3, 701–709 (2020).
16. Heilmayr, R., Rausch, L. L., Munger, J. & Gibbs, H. K. Brazil’s Amazon Soy Moratorium reduced deforestation. *Nature Food* 1, 801–810 (2020).
17. Food and Agriculture Organization (FAO). *Global Forest Resources Assessment 2020: Terms and Definitions*.
18. MacDonald, A. J. & Mordecai, E. A. Amazon deforestation drives malaria transmission, and malaria burden reduces forest clearing. *Proc. Natl. Acad. Sci. USA* 116, 22212–22218 (2019).
19. Vancutsem, C. et al. Long-term (1990–2019) monitoring of forest cover changes in the humid tropics. *Sci. Adv.* 7, eabe1603 (2021).
20. Rudel, T. K., Defries, R., Asner, G. P. & Laurance, W. F. Changing drivers of deforestation and new opportunities for conservation. *Conserv. Biol.* 23, 1396–1405 (2009).
21. Hosonuma, N. et al. An assessment of deforestation and forest degradation drivers in developing countries. *Environ. Res. Lett.* 7, 044009 (2012).
22. Kim, O.-H. et al. Global, Landsat-based forest-cover change from 1990 to 2000. *Remote Sens. Environ.* 155, 178–193 (2014).
23. Curtis, P. G., Slay, C. M., Harris, N. L., Tyukavina, A. & Hansen, M. C. Classifying drivers of global forest loss. *Science* 361, 1108–1111 (2018).
24. Leimgruber, P. et al. Forest cover change patterns in Myanmar (Burma) 1990–2000. *Environ. Conserv.* 32, 356–364 (2005).
25. Stibig, H. J., Achard, F., Carboni, S., Rasi, R. & Miettinen, J. Change in tropical forest cover of Southeast Asia from 1990 to 2010. *Biogeosciences* 11, 247–258 (2014).
26. Ahammad, R., Stacey, N., Eddy, I. M. S., Tomscha, S. A. & Sunderland, T. C. H. Recent trends of forest cover change and ecosystem services in eastern upland region of Bangladesh. *Sci. Total Environ.* 647, 379–389 (2019).
27. Potapov, P., Hansen, M. C., Stehman, S. V., Loveland, T. R. & Pittman, K. Combining MODIS and Landsat imagery to estimate and map boreal forest cover loss. *Remote Sens. Environ.* 112, 3708–3719 (2008).
28. Liu, H. Y. & Yin, Y. Response of forest distribution to past climate change: an insight into future predictions. *Sci. Bull.* 58, 4426–4436 (2013).
29. Shi, L. et al. Decoupled heatwave-tree growth in large forest patches of *Larix sibirica* in northern Mongolian Plateau. *Agr. Forest Meteorol.* 311, 108667 (2021).
30. Tarasov, P. et al. Satellite- and pollen-based quantitative woody cover reconstructions for northern Asia: verification and application to late-Quaternary pollen data. *Earth Planet. Sc. Lett.* 264, 284–298 (2007).
31. Tarasov, P. E., Bezrukova, E. V. & Krivonogov, S. K. Late Glacial and Holocene changes in vegetation cover and climate in southern Siberia derived from a 15 kyr long pollen record from Lake Kotokel. *Clim. Past* 5, 127–151 (2009).

32. Han, Y., Liu, H., Zhou, L., Hao, Q. & Cheng, Y. Postglacial evolution of forest and grassland in southeastern Gobi (Northern China). *Quaternary Sci. Rev.* **248**, 106611 (2020).
33. Liu, X., Jones, M. K., Zhao, Z., Liu, G. & O'Connell, T. C. The earliest evidence of millet as a staple crop: New light on neolithic foodways in North China. *Am. J. Phys. Anthropol.* **149**, 283–290 (2012).
34. Yang, X. Y. et al. Early millet use in northern China. *Proc. Natl Acad. Sci. USA.* **109**, 3726–3730 (2012).
35. Wu, X. et al. Evolution and effects of the social-ecological system over a millennium in China's Loess Plateau. *Sci. Adv.* **6**, eabc0276 (2020).
36. Zhao, Z. J. et al. Flotation results and analysis of plant remains at Donghulin site in Beijing. *Archaeology* **7**, 99–106 (2020). (in Chinese).
37. Wang, C. C. et al. Genomic insights into the formation of human populations in East Asia. *Nature* **591**, 413–419 (2021).
38. Li, Y. Y., Cui, H. T. & Hu, J. M. Analysis for ecological background of ancient civilization in Xiliaohe River Basin. *Quaternary Sci.* **23**, 291–299 (2003). (in Chinese with English abstract).
39. Han, M. *Historical Agricultural Geography of China* (Peking University Press, 2012).
40. Yuan, J. *Research on Subsistence from the Neolithic to the Bronze Age in China* (Fudan University Press, 2019).
41. He, J. et al. Mid-Late Holocene climate change and its impact on the agriculture-pastoralism evolution in the West Liaohe Basin. *Acta Geographica Sinica* **76**, 1618–1633 (2021). (in Chinese with English abstract).
42. An, C. B., Tang, L. Y., Barton, L. & Chen, F. H. Climate change and cultural response around 4000 cal yr BP in the western part of Chinese Loess Plateau. *Quaternary Res.* **63**, 347–352 (2005).
43. Li, Y. Y., Willis, K. J., Zhou, L. P. & Cui, H. T. The impact of ancient civilization on the northeastern Chinese landscape: palaeoecological evidence from the Western Liaohe River Basin, Inner Mongolia. *Holocene* **16**, 1109–1121 (2006).
44. Dykoski, C. A. et al. A high-resolution, absolute-dated Holocene and deglacial Asian monsoon record from Dongge Cave, China. *Earth Planet. Sci. Lett.* **233**, 71–86 (2005).
45. Xu, Q., Xiao, J., Li, Y., Tian, F. & Nakagawa, T. Pollen-based quantitative reconstruction of Holocene climate changes in the Daihai Lake area, Inner Mongolia, China. *J. Climate* **23**, 2856–2868 (2010).
46. Cheng, H. et al. The Asian monsoon over the past 640,000 years and ice age terminations. *Nature* **534**, 640–646 (2016).
47. Cheng, Y. et al. Contrasting effects of winter and summer climate on alpine timberline evolution in monsoon-dominated East Asia. *Quaternary Sci. Rev.* **169**, 278–287 (2017).
48. Williams, J. W., Summers, R. L. & Iii, T. W. Applying plant functional types to construct biome maps from eastern north American pollen data: comparisons with model results. *Quaternary Sci. Rev.* **17**, 607–627 (1998).
49. Breiman, L. Random forests. *Mac. Learn.* **45**, 5–32 (2001).
50. Viau, A. E., Ladd, M. & Gajewski, K. The climate of north America during the past 2000 years reconstructed from pollen data. *Global Planet. Change* **84–85**, 75–83 (2012).
51. Wang, C., Lu, H., Zhang, J., Gu, Z. & He, K. Prehistoric demographic fluctuations in China inferred from radiocarbon data and their linkage with climate change over the past 50,000 years. *Quaternary Sci. Rev.* **98**, 45–59 (2014).
52. Dong, G., Li, R., Lu, M., Zhang, D. & James, N. Evolution of human-environmental interactions in China from the Late Paleolithic to the Bronze Age. *Prog. Phys. Geog.* **44**, 233–250 (2020).
53. Hosner, D., Wagner, M., Tarasov, P. E., Chen, X. & Leipe, C. Spatiotemporal distribution patterns of archaeological sites in China during the Neolithic and Bronze Age: An overview. *Holocene* **26**, 1576–1593 (2016).
54. Li, F. et al. Towards quantification of Holocene anthropogenic land-cover change in temperate China: a review in the light of pollen-based REVEALS reconstructions of regional plant cover. *Earth-Sci. Rev.* **203**, 103119 (2020).
55. Yang, B. et al. Long-term decrease in Asian monsoon rainfall and abrupt climate change events over the past 6,700 years. *Proc. Natl Acad. Sci. USA.* **118**, e2102007118 (2021).
56. Zhao, W. L. & Xie, S. J. *Population history of China* (People's Publishing House, 1988).
57. Ge, J. X. *Population History of China* (Fudan University Press, 2002).
58. Jin, Y. Q. War between Song and Xia and grassland changes in central and western of Loess Plateau. *J. Arid Land Resour. Environ.* **24**, 192–195 (2010). (in Chinese with English abstract).
59. Atahan, P. et al. Holocene-aged sedimentary records of environmental changes and early agriculture in the lower Yangtze, China. *Quaternary Sci. Rev.* **27**, 556–570 (2008).
60. Xu, X., Li, F., Lin, Z. & Song, X. Holocene fire history in China: Responses to climate change and human activities. *Sci. Total Environ.* **753**, 142019 (2021b).
61. Kukla, T. et al. The resilience of Amazon tree cover to past and present drying. *Glob. Planet. Change* **202**, 103520 (2021).
62. Williams, J. W., Tarasov, P., Brewer, S. & Notaro, M. Late-Quaternary variations in tree cover at the northern forest-tundra ecotone. *J. Geophys. Res.-Bioge.* **116**, G1017 (2011).
63. Woodbridge, J., Fyfe, R. M. & Roberts, N. A. comparison of remote-sensed and pollen-based approaches to mapping Europe's land cover. *J. Biogeogr.* **41**, 2080–2092 (2014).
64. Trondman, A. K. et al. Pollen-based quantitative reconstructions of Holocene regional vegetation cover (plant-functional types and land-cover types) in Europe suitable for climate modelling. *Global Change Biol.* **21**, 676–697 (2015).
65. Shennan, S. et al. Regional population collapse followed initial agriculture booms in mid-Holocene Europe. *Nat. Commun.* **4**, 2486 (2013).
66. Roberts, N. et al. Europe's lost forests: a pollen-based synthesis for the last 11,000 years. *Sci. Rep.-UK* **8**, 716 (2018).
67. Zhai, D. L., Xu, J. C., Dai, Z. C., Cannon, C. H. & Grumbine, R. E. Increasing tree cover while losing diverse natural forests in tropical Hainan, China. *Reg. Environ. Change* **14**, 611–621 (2014).
68. de Rezende, C. L., Uezu, A., Scarano, F. R. & Araujo, D. S. D. Atlantic Forest spontaneous regeneration at landscape scale. *Biodivers. Conserv.* **24**, 2255–2272 (2015).
69. Borda-Nino, M., Meli, P. & Brancalion, P. H. S. Drivers of tropical forest cover increase: a systematic review. *Land Degrad. Dev.* **31**, 1366–1379 (2020).
70. Bennie, J., Huntley, B., Wiltshire, A., Hill, M. O. & Baxter, R. Slope, aspect and climate: spatially explicit and implicit models of topographic micro-climate in chalk grassland. *Ecol. Model.* **216**, 47–59 (2008).
71. Burnett, B. N., Meyer, G. A. & McFadden, L. D. Aspect-related microclimatic influences on slope forms and processes, northeastern Arizona. *J. Geophys. Res.-Earth* **113**, F03002 (2008).
72. Moeslund, J. E. et al. Topographically controlled soil moisture is the primary driver of local vegetation patterns across a lowland region. *Ecosphere* **4**, 91 (2013).
73. Peng, C. et al. A drought-induced pervasive increase in tree mortality across Canada's boreal forests. *Nat. Clim. Change* **1**, 467–471 (2011).
74. Liu, H. Y. et al. Rapid warming accelerates tree growth decline in semi-arid forests of Inner Asia. *Global Change Biol.* **19**, 2500–2510 (2013).
75. Williams, A. P. et al. Temperature as a potent driver of regional forest drought stress and tree mortality. *Nat. Clim. Change* **3**, 292–297 (2013).
76. Liu, H. Y. It is difficult for China's greening through large-scale afforestation to cross the Hu Line. *Sci. China Earth Sci.* **62**, 1662–1664 (2019).
77. Romero-Diaz, A., Belmonte-Serrato, F. & Ruiz-Sinoga, J. D. The geomorphic impact of afforestations on soil erosion in southeast Spain. *Land Degrad. Dev.* **21**, 188–195 (2010).
78. Li, H., Si, B. & Li, M. Rooting depth controls potential groundwater recharge on hillslopes. *J. Hydrol.* **564**, 164–174 (2018).
79. Liu, H. Y., Yin, Y., Zhu, J. L., Zhao, F. J. & Wang, H. Y. How did the forest respond to Holocene climate drying at the forest-steppe ecotone in northern China? *Quatern. Int.* **227**, 46–52 (2010).
80. Hao, Q., Liu, H., Yin, Y., Wang, H. & Feng, M. Varied responses of forest at its distribution margin to Holocene monsoon development in northern China. *Palaeogeogr. Palaeoclimatol.* **409**, 239–248 (2014).
81. Liu, H. Y., Yin, Y., Hao, Q. & Liu, G. Sensitivity of temperate vegetation to Holocene development of East Asian monsoon. *Quaternary Sci. Rev.* **98**, 126–134 (2014).
82. Zhang, P. et al. China's forest policy for the 21st century. *Science* **288**, 2135–2136 (2000).
83. Liu, Z. et al. Transient simulation of last deglaciation with a new mechanism for Bolling-Allerod warming. *Science* **325**, 310–314 (2009).
84. He, F. *Simulating transient climate evolution of the last deglaciation with CCSM3* (Bern Switzerland Pages International Program Office, 2011).
85. Marlon, J. R. et al. Global biomass burning: a synthesis and review of Holocene paleofire records and their controls. *Quaternary Sci. Rev.* **65**, 5–25 (2013).
86. Zhang, D. L., Huang, X. Z., Liu, Q., Chen, X. & Feng, Z. D. Holocene fire records and their drivers in the westerlies-dominated Central Asia. *Sci. Total Environ.* **833**, 155153 (2022).
87. Davis, M. B. On the theory of pollen analysis. *Am. J. Sci.* **261**, 897–912 (1963).
88. Parsons, R. W. & Prentice, I. C. Statistical approaches to R-Values and the pollen-vegetation relationship. *Rev. Palaeobot. Palyno.* **32**, 127–152 (1981).
89. Prentice, I. C. & Parsons, R. W. Maximum likelihood linear calibration of pollen spectra in terms of forest composition. *Biometrics* **39**, 1051–1057 (1983).
90. Hellman, S., Gaillard, M., Broström, A. & Sugita, S. The REVEALS model, a new tool to estimate past regional plant abundance from pollen data in large lakes: validation in southern Sweden. *J. Quaternary Sci.* **23**, 21–42 (2008).
91. Gaillard, M. J. et al. Holocene land-cover reconstructions for studies on land cover-climate feedbacks. *Clim. Past* **6**, 483–499 (2010).
92. Soepboer, W., Sugita, S. & Lotter, A. F. Regional vegetation-cover changes on the Swiss Plateau during the past two millennia: a pollen-based reconstruction using the REVEALS model. *Quaternary Sci. Rev.* **29**, 472–483 (2010).



93. Cui, Q. Y. et al. Historical land-use and landscape change in southern Sweden and implications for present and future biodiversity. *Eco. Evol.* **4**, 3555–3570 (2014).
94. Theuerkauf, M., Couwenberg, J., Kuparinen, A. & Liebscher, V. A matter of dispersal: REVEALSinR introduces state-of-the-art dispersal models to quantitative vegetation reconstruction. *Veg. Hist. Archaeobot.* **25**, 541–553 (2016).
95. Sobol, M. K. & Finkelstein, S. A. Predictive pollen-based biome modeling using machine learning. *PLoS ONE* **13**, e0202214 (2018).
96. Oliveira, S., Oehler, F., San-Miguel-Ayanz, J., Camia, A. & Pereira, J. M. C. Modeling spatial patterns of fire occurrence in Mediterranean Europe using Multiple Regression and Random Forest. *Forest Ecol. Manag.* **275**, 117–129 (2012).
97. Prasad, A. M., Iverson, L. R. & Liaw, A. Newer classification and regression tree techniques: bagging and random forests for ecological prediction. *Ecosystems* **9**, 181–199 (2006).
98. Cutler, D. R. et al. Random forests for classification in ecology. *Ecology* **88**, 2783–2792 (2007).
99. Qin, F., Zhao, Y. & Cao, X. Y. Biome reconstruction on the Tibetan Plateau since the Last Glacial Maximum using a machine learning method. *Sci. China Earth Sci.* **65**, 518–535 (2022).
100. Liu, H. Y. et al. Topography-controlled soil water content and the coexistence of forest and steppe in northern China. *Phys. Geogr.* **33**, 561–573 (2012).

### Acknowledgements

This work was supported by the Key Project of the Ministry of Science and Technology of China [grant number 2022YFF0801803].

### Author contributions

Q.H. analyzed the data and wrote the manuscript. Y.H. collected and analysed the data. H.L. designed this study. Y.C. collected the data. All authors revised and approved the final manuscript.

### Competing interests

The authors declare no competing interests.

### Additional information

**Supplementary information** The online version contains supplementary material available at <https://doi.org/10.1038/s43247-023-00814-5>.

**Correspondence** and requests for materials should be addressed to Hongyan Liu.

**Peer review information** *Communications Earth & Environment* thanks Feng-Min Li, Hou Guolong, Ting Ma, and Xiaolin Ren for their contribution to the peer review of this work. Primary Handling Editor: Aliénor Lavergne. Peer reviewer reports are available.

**Reprints and permission information** is available at <http://www.nature.com/reprints>

**Publisher's note** Springer Nature remains neutral with regard to jurisdictional claims in published maps and institutional affiliations.



**Open Access** This article is licensed under a Creative Commons Attribution 4.0 International License, which permits use, sharing, adaptation, distribution and reproduction in any medium or format, as long as you give appropriate credit to the original author(s) and the source, provide a link to the Creative Commons license, and indicate if changes were made. The images or other third party material in this article are included in the article's Creative Commons license, unless indicated otherwise in a credit line to the material. If material is not included in the article's Creative Commons license and your intended use is not permitted by statutory regulation or exceeds the permitted use, you will need to obtain permission directly from the copyright holder. To view a copy of this license, visit <http://creativecommons.org/licenses/by/4.0/>.

© The Author(s) 2023